# Reduced Water Vapor Transmission Rate of Graphene Gas Barrier Films for Flexible Organic Field-Effect Transistors

Kyoungjun Choi,[†,¶] Sooji Nam,[‡,§,¶] Youngbin Lee,[⊥,¶] Mijin Lee,[∥] Jaeyoung Jang,[‡,#] Sang Jin Kim,[†] Yong Jin Jeong,[‡] Hyeongkeun Kim,[▽] Sukang Bae,[⊗] Ji-Beom Yoo,[⊥,△] Sung M. Cho,[⊥,○] Jae-Boong Choi,[⊥,□] Ho Kyoon Chung,[⊥] Jong-Hyun Ahn,*[⌐] Chan Eon Park,*[‡] and Byung Hee Hong*[†]

[†]Department of Chemistry, College of Natural Sciences Seoul National University, Gwanakro-1, Seoul 151-747, Republic of Korea, [‡]Polymer Research Institute, Department of Chemical Engineering, Pohang University of Science and Technology (POSTECH), Pohang 790-784, Korea, [§]Smart I/O Control Device Research Section, Electronics and Telecommunications Research Institute, 218 Gajeong-ro, Yuseong-gu, Daejeon 305-700, South Korea, [⊥]SKKU Advanced Institute of Nanotechnology (SAINT) and Center for Human Interface Nano Technology (HINT), Sungkyunkwan University, Suwon 440-746, Korea, [∥]Future Technology Research Center Corporate R&D, LG Chem Research Park, Daejeon 305-738, Korea, [#]Department of Energy Engineering, Hanyang University, Seoul 133-791, Republic of Korea, [▽]Electronic Materials & Device Research Center, Korea Electronics Technology Institute, Saenari-ro, Bundang-gu, Seongnam-si, Gyeonggi-do 463-816, Korea, [⊗]Institute of Advanced Composite Materials, Korea Institute of Science and Technology, Eunha-ri san 101, Bongdong-eup, Wanju-gun, Jeollabukdo (or Jeonbuk) 565-905, Republic of Korea, [□]School of Mechanical Engineering, [△]School of Advanced Materials Science and Engineering, [○]School of Chemical Engineering, and Department of Chemistry, Sungkyunkwan University, Suwon 440-746, Korea, and [⌐]School of Electrical and Electronic Engineering, Yonsei University, Seoul 120-749, Korea. [¶]These authors contributed equally to this work.

ABSTRACT Preventing reactive gas species such as oxygen or water is important to ensure the stability and durability of organic electronics. Although inorganic materials have been predominantly employed as the protective layers, their poor mechanical property has hindered the practical application to flexible electronics. The densely packed hexagonal lattice of carbon atoms in graphene does not allow the transmission of small gas molecules. In addition, its outstanding

mechanical flexibility and optical transmittance are expected to be useful to overcome the current mechanical limit of the inorganic materials. In this paper, we reported the measurement of the water vapor transmission rate (WVTR) through the 6-layer 10×10 cm^2 large-area graphene films synthesized by chemical vapor deposition (CVD). The WVTR was measured to be as low as 10^{-4} g/m$^2 \cdot$day initially, and stabilized at ~0.48 g/m$^2 \cdot$day, which corresponds to 7 times reduction in WVTR compared to bare polymer substrates. We also showed that the graphene-passivated organic field-effect transistors (OFETs) exhibited excellent environmental stability as well as a prolonged lifetime even after 500 bending cycles with strain of 2.3%. We expect that our results would be a good reference showing the graphene's potential as gas barriers for organic electronics.
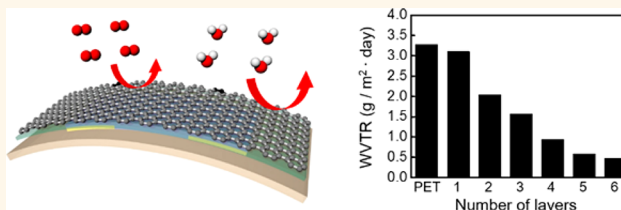
KEYWORDS: graphene barrier · water vapor transmittance rate · OFETs · bending cycles

G raphene, an atomically thin two-dimensional carbon allotrope with hexagonal lattice structures, has been intensively studied in recent years owing to its outstanding electrical,[1−3] mechanical,[4,5] and chemical properties.[6,7] In particular, graphene has received much attention as a promising barrier material not only because of its densely packed structure that does not allow the transmission of gases or liquids[8−17] but also because of outstanding optical transparency and mechanical flexibility. This is particularly important for flexible organic field-effect transistors (OFETs),[18−21] as the performance of organic materials considerably

degrades in the presence of water or oxygen molecules from ambient air.[22−24] Inorganic materials such as silicone oxides (SiOx) and aluminum oxides (Al$_2$O$_3$) have been predominantly employed as the gas barrier films.[25−27] However, the complicated fabrication processes as well as the poor mechanical flexibility of these materials have hindered the practical application to flexible electronic devices.[28,29] In this regard, the excellent gas-impermeability, flexibility, and transmittance of graphene films[30] are expected to be useful for more reliable and durable operation of organic devices. Recently, Lange et al. have discovered the impermeable characteristics

of mechanically exfoliated graphene,[31] and Liu et al. have successfully demonstrated the application of large-area graphene films to gas-impermeable top electrodes covering organic photovoltaic devices.[11] However, the impermeability of large-area graphene has not been directly evidenced by measuring the water vapor transmission rate (WVTR), although it is a standard parameter showing the performance of gas-impermeability.

Here, we directly evaluated the gas barrier performance of large-area graphene films (10×10 cm^2) synthesized by chemical vapor deposition (CVD) by measuring the WVTR. The WVTR value of 6-layer graphene on PET films was as low as 10^{-4} g/m^2·day for the first few hours. However, it was gradually increased and stabilized at 0.48 g/m^2·day, which is 7 times lower than bare PET films. The graphene-passivated OFETs exhibit excellent environmental stability as well as a prolonged lifetime compared to the nonpassivated devices even after 500 bending cycles with strain of 2.3%.

RESULTS AND DISCUSSION

We synthesized large-area graphene using a typical CVD method using 35-μm-thick Cu foils with flowing 35 sccm methane and 5 sccm hydrogen gases at 1000 °C,[3] followed by coating with poly(methylmethacrylate) (PMMA) and transfer to PET films. After the removal of PMMA with acetone, considerable amount of PMMA residues remains on graphene surface, which disturbs the close contact between multitransferred graphene layers. Therefore, the PMMA-assisted transfer steps need to be minimized for less polymer residues and for better performance of graphene gas barrier films. Figure 1 shows the difference between a single PMMA coating/removal step (upper) and multiple PMMA coating/removal steps (lower). In the case of conventional transfer processes that includes multiple PMMA coating/removal steps, PMMA/graphene is transferred onto target substrate such

as PET, and then PMMA is removed in acetone. Thus, repetition of PMMA coating/removal steps is needed to obtain multiple stacked graphene. However, in case of single PMMA coating/removal step, PMMA/graphene is directly transferred onto graphene/Cu foil (G/Cu). After etching Cu foil and transferring on G/Cu several times, multiple stacked graphene can be obtained without polymer residue, with only single PMMA removal step. Thus, we used a graphene transfer method that requires only one time use of the PMMA layer as shown in Figure 1.[32]

In the multiple PMMA coating/removal steps, the greater amount of polymer residues remained on graphene compared to the case of using a single PMMA coating/removal step, as evidenced by atomic force microscopy (AFM) and scanning electron microscopy (SEM) images (Figure 2a–d). As a result, the WVTR of the single-PMMA-coated graphene films decreased from 2.22 to 0.94 g/m^2·day, indicating that minimizing the gap between graphene layers efficiently blocks the penetrating passage of water and oxygen molecules. It should be noted that the graphene barrier films initially showed WVTR as low as 10^{-4} g/m^2·day, but the WVTR value gradually increased with time possibly due to the horizontal diffusion of water molecules between the graphene layers (Supporting Information Figure S1). All the WVTR values in the manuscript were measured after the WVTR change has been stabilized and saturated.

The WVTR of monolayer graphene on a PET film (3.11 g/m^2·day) does not much differ from that of a bare PET film (3.28 g/m^2·day) because of defects or tears formed during growth and transfer steps (Supporting Information Figure S2a,b). However, the WVTR considerably decreased by adding another layer of graphene on top (Figure 2f), as the additional layer can patch the defects on the previous graphene layer (Supporting Information Figure S2c). The WVTR of the 6-layer graphene film prepared on a PET substrate was measured to be of 0.48 g/m^2·day, which is 7-fold lower
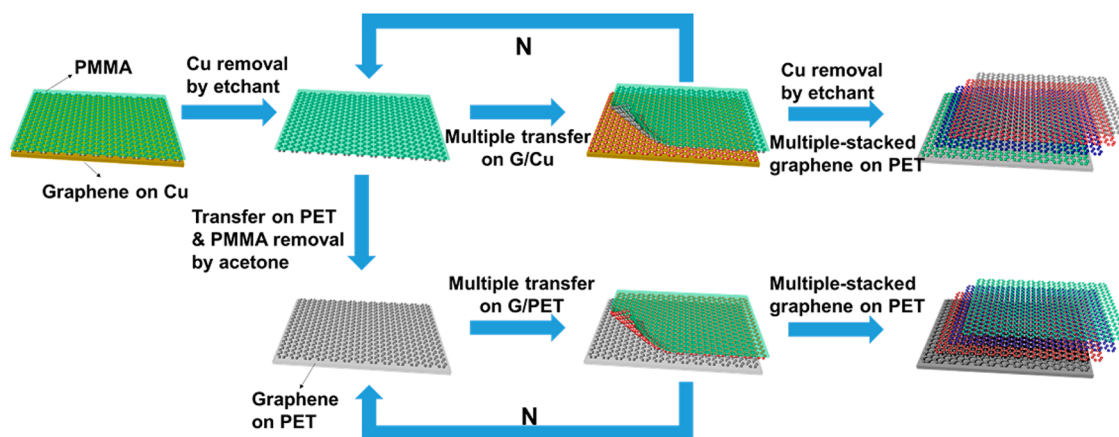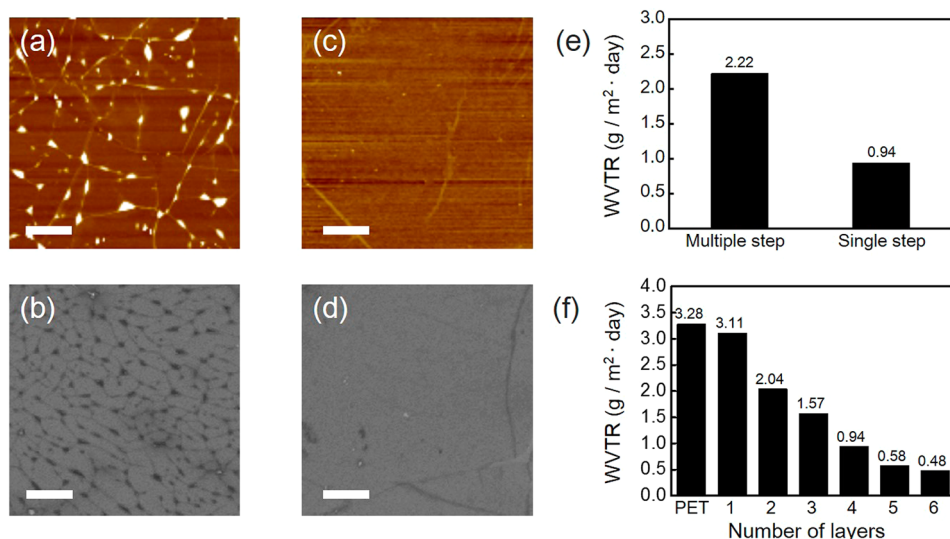

Figure 1. A schematic representation showing the multiple graphene transfer processes that use only a single PMMA removal step (upper) and multiple PMMA removal steps (lower).

Figure 2. (a−d) AFM and SEM images of multilayer graphene transferred by the single PMMA removal step (a and b) and the multiple PMMA removal step (c and d). Scale bars, 1 μm. (e) WVTR values of 4-layer graphene transferred by the multiple/single use of PMMA coating. (f) WVTR values of graphene transferred on a PET film with respect to increasing number of graphene layers at 23 °C and 100% relative humidity.
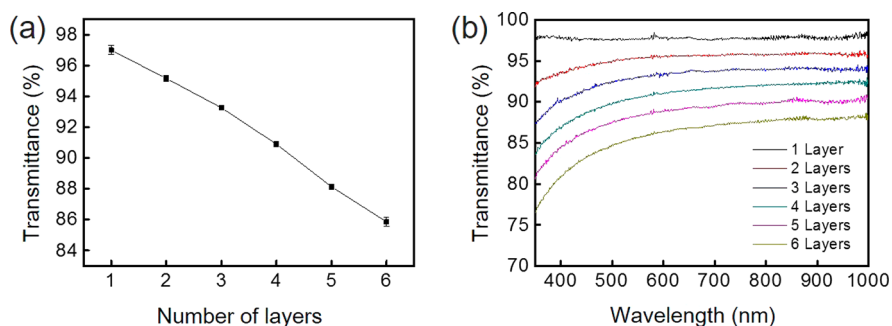
Figure 3. (a and b) Optical transmittance and UV−vis spectra of graphene films on PET films with increasing number of graphene layers, respectively.
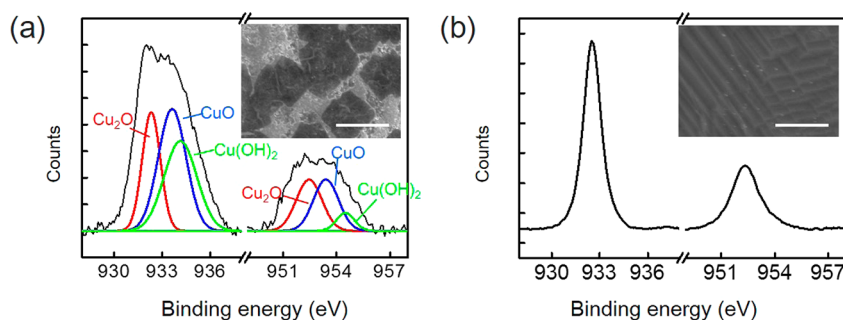

Figure 4. XPS spectra of (a) bare Cu foil and (b) Cu foil with graphene film after air oxidation (Cu 2p$_{3/2}$, 932.6 eV; Cu 2p$_{1/2}$, 952.4 eV; Cu$_2$O, 932.4 and 952.4 eV; CuO, 933.6 and 953.4 eV; Cu(OH)$_2$, 934.3 and 954.5 eV) after two months under ambient pressure and room temperature. Scale bars, 2 μm.

than that of a bare PET film. It should be noted that the 6-layer graphene exhibits an excellent optical transmittance as high as 85% at a wavelength of 550 nm (Figure 3), which is of great importance for the barrier application to various optoelectronic applications.

As mentioned earlier, graphene can act as antioxidation layer because of its densely packed structure

that does not allow the transmission of gases or liquids. We carried out other research on a long-term corrosion protection. As-grown graphene on Cu surface exposed to ambient conditions showed no significant change for more than 2 months, while the bare Cu surface is readily oxidized (Figure 4).[33] XPS spectra of Cu foil with graphene indicate two sharp peaks related to
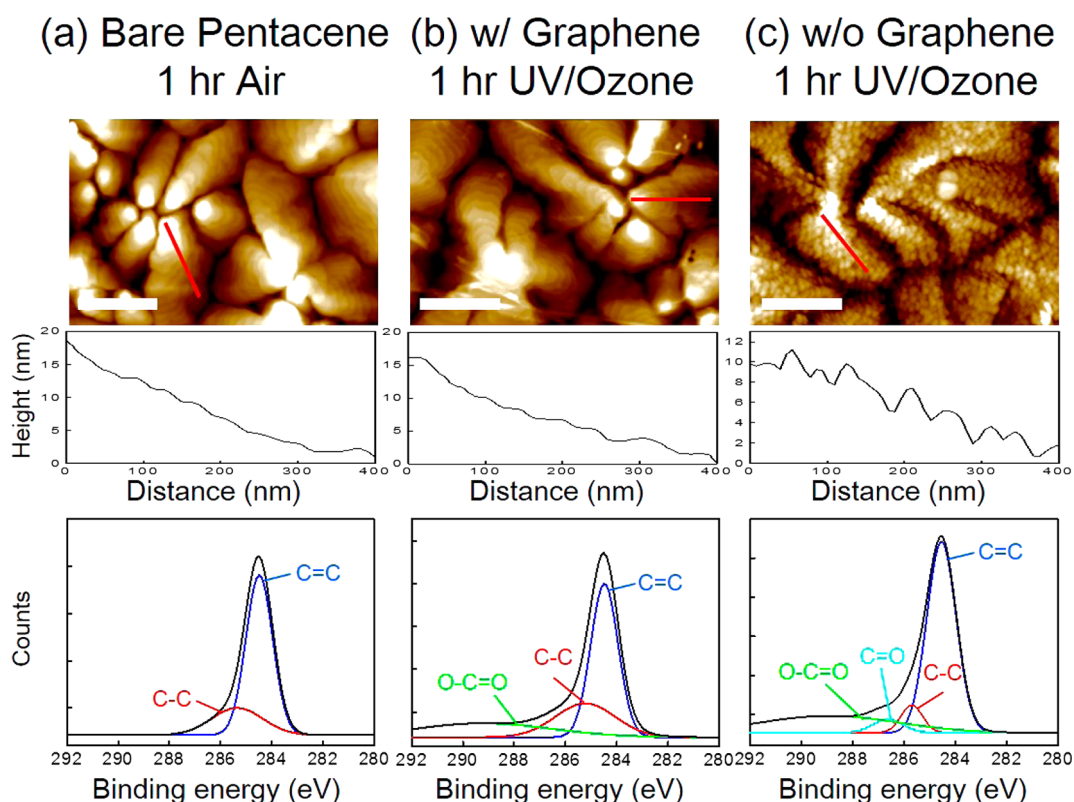
Figure 5. (a−c) AFM topographs and XPS spectra of bare pentacene, oxidized pentacene with graphene, and oxidized pentacene without graphene, respectively. Scale bars, 400 nm. The oxidation was carried out by using UV/ozone treatment for 1 h. The AFM profiles of pentacene on SiO$_2$/Si along the red line clearly shows the degradation of pentacene film by oxidation. The XPS analyses of the C 1s core level bands show that the oxygen related peaks appear as oxidation proceeds.

Cu (Cu 2p$_{3/2}$, 932.6 eV; Cu 2p$_{1/2}$, 952.4 eV), whereas those of bare Cu foil show the broad peaks corresponding to copper oxide (Cu$_2$O, 932.4 and 952.4 eV; CuO, 933.6 and 953.4 eV; Cu(OH)$_2$, 934.3 and 954.5 eV). Therefore, these results suggest that graphene films can defend metals against environment oxidants.

To meet the demands of the growing interest in flexible electronics, organic semiconductors have been intensively studied as emerging materials due to high field-effect mobility and outstanding on−off ratio. Among them, pentacene is a widely used *p*-type organic semiconductor;[34,35] however, its electrical properties, morphology, and chemical states are significantly degraded in the presence of water or oxygen species from ambient air.[36,37] Thus, we investigated the barrier effects of our multistacked graphene by the use of practical pentacene−FET devices on flexible substrates.[20] Stability tests under harsh oxygen-rich conditions were conducted by applying UV/ozone treatment (λ = 254 nm) to the pentacene films. The AFM image shows the typical three-dimensional pyramidal structure of a bare pentacene film on a SiO$_2$ substrate (Figure 5a). As the UV/ozone treatment proceeds, the continuous pentacene film changed to spherical particles and then gradually disappeared (Supporting Information Figure S3).

The AFM images, line profiles, and XPS spectra of a pentacene film on a SiO$_2$/Si substrate in Figure 5 clearly show the difference between UV/ozone-treated pentacene films with and without protecting graphene films. The morphology of the pentacene without protecting graphene became very rough after oxidation. The XPS spectra also indicate that the pentacene unprotected by graphene is easily oxidized while the graphene barrier layer prevents the pentacene from oxidation that leads to the degradation of its semiconducting property. We suppose that a new peak arising at 289 eV (O=C−O), including two conspicuous peaks of bare pentacene films, one strong peak centered at 284.5 eV (C=C) and a sub-band centered at 285.7 eV (C−C), in Figure 5b result from PMMA residues on top of the protecting graphene layer and the appearance of the oxygen-containing groups on the graphene surface; thus, the underlying pentacene is still safe from the harsh oxidation condition (AFM image in Figure 5b). As shown in Figure 5c, the new peaks corresponding to C−C, O=C−O, and 287.6 eV (C=O) groups reveal that the pentacene film without a graphene barrier has been heavily oxidized,[22] which is also in good agreement with a previous report that showed the deformed surface morphology of oxidized pentacene films after UV irradiation in the presence of oxygen species (Supporting Information Figure S3).

The barrier robustness of the graphene films was further verified by applying these to OFETs.
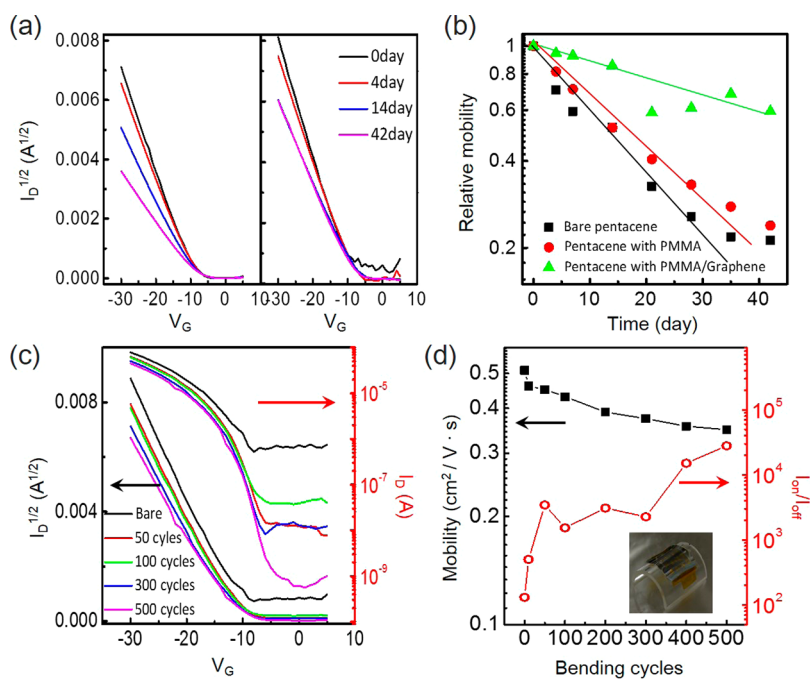
Figure 6. (a) Time-dependent $I_D^{1/2}$ *vs* V_G characteristics of the bare OFETs (left) and an OFET passivated with PMMA/graphene (right). (b) Time-dependent relative field-effect mobilities of bare pentacene, pentacene with PMMA, and pentacene with PMMA/graphene films. Bending cycle tests: (c) I_D *vs* V_G transfer characteristics and the $I_D^{1/2}$ *versus* V_G characteristics of a passivated OFET prepared with PMMA/6-layer graphene. (d) Field-effect mobility and on−off ratio of a passivated OFET prepared with PMMA/6-layer graphene. All the electrical measurements were performed using the reversed transfer method at 25 °C under 60% relative humidity.

The field-effect mobilities of the OFETs were obtained from the slope of a plot of the square root of the drain current (I_D) *versus* the gate voltage (V_G) in the saturation current region using the following equation:

$$I_D = \left(\frac{WC_i}{2L}\right)\mu(V_G - V_{th})^2$$

where I_D is the drain current, C_i is the capacitance per unit area of the dielectric, and W and L are the channel width and length, respectively. In case of direct contact between graphene and pentacene, the pentacene of the channel region can be seriously damaged due to the overflow of charges through graphene (Supporting Information Figure S5c). To avoid this problem induced by the conductivity of graphene barrier layers, the PMMA side of the PMMA/graphene film needs to be in contact with the pentacene layer, which can be accomplished by a reversed transfer method as depicted in Supporting Information Figure S4.[38] PMMA as a dielectric layer can block vertical overflow through the graphene layer.[39] We fabricated a device with a structure containing polyarylate (PAR)/Al/Al$_2$O$_3$/Au/pentacene/PMMA/graphene (a mobility of ∼0.5 cm$^2 \cdot$V$^{-1} \cdot$s^{-1} in Supporting Information Figure S5a). Figure 6 shows the characteristics of OFET as time passed and bending stability, respectively. The devices were kept in a 60 °C and 60% relative humidity conditioned chamber. The $I_D^{1/2}$ *versus* V_G and relative mobility of graphene-passivated OFETs changed much less than the unpassivated OFETs with the elapse of time (Figure 6a,b).
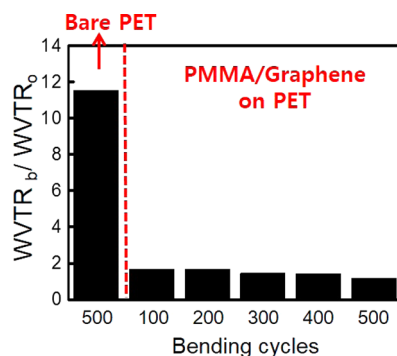
Figure 7. Relative WVTR values with increasing bending cycles, where WVTR$_o$ and WVTR$_b$ denote the WVTR values before and after bending, respectively.

We also evaluated the stability of the graphene passivation layer by monitoring the OFET performance with respect to cyclic bending at ∼2.3% strain, resulting in only ∼30% degradation in mobility (from 0.51 ± 0.04 to 0.35 ± 0.09 cm$^2 \cdot$V$^{-1} \cdot$s^{-1}) but considerable enhancement in on/off ratios (Figure 6c,d). This result well matches with the stable WVTR values of bended graphene/PET films (Figure 7). The WVTR of the PET after 500-cycle bending test increased by a factor of 10 compared to PET prior to bending, whereas the barrier properties of graphene/PET films were gradually stabilized with bending cycles. We suppose that the poor off-current problem in graphene-passivated OFETs can be removed if wrinkles and voids that are unfavorable for the dielectric property

of PMMA/graphene layers disappear with cyclic bending. We further infer that graphene is a very effective barrier film regardless of the number of bending cycles.

CONCLUSIONS

In summary, we have successfully measured the WVTR of large-area graphene films grown by CVD, which is as low as 0.48 g/m^2·day corresponding to a 7-fold improvement compared to a bare PET film. The AFM images and XPS spectra revealed that the graphene films efficiently protect a pentacene film from oxidizing species. We also showed that the flexible OFETs passivated with the graphene films exhibit prolonged lifetimes (~42 days) and mechanical stability over 500 bending cycles (~2.3% strain). We believe that our results provide an important reference that supports the excellent gas barrier properties of large-area graphene films, but further optimization is needed to fully utilize the intrinsic gas-impermeable capability of graphene films.

EXPERIMENTAL SECTION

Sample Preparation. Monolayer graphene was grown on a Cu foil in a quartz tube using CVD methods. The Cu foil was heated at 1000 °C for 1 h under a 5 sccm H$_2$ flow, and then 35 sccm CH$_4$ was inserted to permit graphene growth over 30 min. Finally, the furnace was rapidly cooled to room temperature under a H$_2$ flow. To protect the graphene, the PMMA solution was applied onto the graphene/Cu foil using a spin-coater. The Cu foil was etched away using 0.05 M ammonium persulfate over 7 h. The floating graphene layer and the PMMA support film were transferred onto the target substrate.

A 50 nm-thick Al layer was deposited onto a PAR substrate to form a gate electrode. Subsequently, a 100 nm-thick Al$_2$O$_3$ layer was coated as a gate insulator using a plasma enhanced atomic layer deposition (PEALD) process. During the PEALD process, trimethylaluminum (TMA) and oxygen (O$_2$) gases were used as the sources of Al and O, respectively. The PEALD process is described in detail elsewhere.[40] A 30 nm layer of a cyclic olefin copolymer (Polyscience Co.) was spin-coated to provide a bilayer gate dielectric layer. The samples were then heated on a 120 °C hot plate for 30 min to remove residual solvent. Subsequently, a 50 nm-thick pentacene film was deposited onto the dielectric layer by means of organic molecular beam deposition under high vacuum (i.e., 10^{-7} Torr) at a rate of 0.2 Å/s through a shadow mask. The top-contact geometry was prepared by thermally evaporating gold source/drain electrodes through a shadow mask onto the pentacene layer (5 Å/s under 10^{-6} Torr). The channel length (L) and width (W) of the shadow mask used for the gold deposition step were fixed at 100 and 1500 μm, respectively.

Characterization. The transmittances of graphene were measured using a SINCO S-3100. The surfaces of the graphene were imaged using a field-emission scanning electron microscope (AURIGA, Carl Zeiss). The AFM images were collected in the noncontact mode using a Park System XE-100 atomic force microscope. The C 1s core level bands of graphene were acquired using an Axis-HIS (Kratos, Inc.). Water vapor transmission rate (WVTR) testing was performed in accordance with the ASTM F1249, using a PERMATRAN_W 3/33 MA (MOCON) at room temperature and 100% RH. (Film type of barrier materials is placed in test cell, which is made up inside chamber and outside chamber and separated by test sample. The inside chamber is filled with nitrogen (carrier gas) and the outside chamber is filled with water vapor (test gas). Molecules of water diffuse through the test film to the inside chamber and are conveyed to the sensor by the carrier gas. The computer monitors the increase in water vapor concentration in the carrier gas and it reports that value on the screen as the water vapor transmission rate.) The electrical characteristics of the pentacene FETs were measured using Keithley 2400 and 236 source/measure units. The capacitances were characterized using a 4284A LCR meter (Agilent Tech).

Conflict of Interest: The authors declare no competing financial interest.

Supporting Information Available: Additional SEM, AFM, electrical, and WVTR data. The Supporting Information is available free of charge on the ACS Publications website at DOI: 10.1021/acsnano.5b01161.

REFERENCES AND NOTES

1. Geim, A. K.; Novoselov, K. S. The Rise of Graphene. *Nat. Mater.* **2007**, *6*, 183–191.
2. Bolotin, K. I.; Sikes, K. J.; Jiang, Z.; Klima, M.; Fudenberg, G.; Hone, J.; Kim, P.; Stormer, H. L. Ultrahigh Electron Mobility in Suspended Graphene. *Solid State Commun.* **2008**, *146*, 351–355.
3. Bae, S.; Kim, H.; Lee, Y.; Xu, X.; Park, J.-S.; Zheng, Y.; Balakrishnan, J.; Lei, T.; Ri Kim, H.; Song, Y. I. Roll-to-roll Production of 30-in. Graphene Films for Transparent Electrodes. *Nat. Nanotechnol.* **2010**, *5*, 574–578.
4. Lee, C.; Wei, X.; Kysar, J. W.; Hone, J. Measurement of the Elastic Properties and Intrinsic Strength of Monolayer Graphene. *Science* **2008**, *321*, 385–388.
5. Koenig, S. P.; Boddeti, N. G.; Dunn, M. L.; Bunch, J. S. Ultrastrong Adhesion of Graphene Membranes. *Nat. Nanotechnol.* **2011**, *6*, 543–546.
6. McAllister, M. J.; Li, J.-L.; Adamson, D. H.; Schniepp, H. C.; Abdala, A. A.; Liu, J.; Herrera-Alonso, M.; Milius, D. L.; Car, R.; Prud'homme, R. K. Single Sheet Functionalized Graphene by Oxidation and Thermal Expansion of Graphite. *Chem. Mater.* **2007**, *19*, 4396–4404.
7. Wang, X.; Li, X.; Zhang, L.; Yoon, Y.; Weber, P. K.; Wang, H.; Guo, J.; Dai, H. n-Doping of Graphene through Electrothermal Reactions with Ammonia. *Science* **2009**, *324*, 768–771.
8. Bunch, J. S.; Verbridge, S. S.; Alden, J. S.; van der Zande, A. M.; Parpia, J. M.; Craighead, H. G.; McEuen, P. L. Impermeable Atomic Membranes from Graphene Sheets. *Nano Lett.* **2008**, *8*, 2458–2462.
9. Nair, R. R.; Wu, H. A.; Jayaram, P. N.; Grigorieva, I. V.; Geim, A. K. Unimpeded Permeation of Water through Helium-Leak—Tight Graphene-Based Membranes. *Science* **2012**, *335*, 442–444.
10. Shin, D.; Park, J. B.; Kim, Y.-J.; Kim, S. J.; Kang, J. H.; Lee, B.; Cho, S.-P.; Hong, B. H.; Novoselov, K. S. Growth Dynamics and Gas Transport Mechanism of Nanobubbles in Graphene Liquid Cells. *Nat. Commun.* **2015**, *6*, No. 6068.
11. Liu, Z.; Li, J.; Yan, F. Package-Free Flexible Organic Solar Cells with Graphene top Electrodes. *Adv. Mater.* **2013**, *25*, 4296–4301.

12. Zhao, Y.; Xie, Y.; Hui, Y. Y.; Tang, L.; Jie, W.; Jiang, Y.; Xu, L.; Lau, S. P.; Chai, Y. Highly Impermeable and Transparent Graphene as an Ultra-Thin Protection Barrier for Ag Thin Films. *J. Mater. Chem. C* **2013**, *1*, 4956–4961.

13. Su, Y.; Kravets, V. G.; Wong, S. L.; Waters, J.; Geim, A. K.; Nair, R. R. Impermeable Barrier Films and Protective Coatings Based on Reduced Graphene Oxide. *Nat. Commun.* **2014**, *5*, No. 4843.

14. Yamaguchi, H.; Granstrom, J.; Nie, W.; Sojoudi, H.; Fujita, T.; Voiry, D.; Chen, M.; Gupta, G.; Mohite, A. D.; Graham, S. Reduced Graphene Oxide Thin Films as Ultrabarriers for Organic Electronics. *Adv. Energy Mater.* **2014**, *4*, 1300986.

15. Celebi, K.; Buchheim, J.; Wyss, R. M.; Droudian, A.; Gasser, P.; Shorubalko, I.; Kye, J.-I.; Lee, C.; Park, H. G. Ultimate Permeation Across Atomically Thin Porous Graphene. *Science* **2014**, *344*, 289–292.

16. Boutilier, M. S. H.; Sun, C.; O'Hern, S. C.; Au, H.; Hadjiconstantinou, N. G.; Karnik, R. Implications of Permeation through Intrinsic Defects in Graphene on the Design of Defect-Tolerant Membranes for Gas Separation. *ACS Nano* **2014**, *8*, 841–849.

17. Yang, S.; Zhan, L.; Xu, X.; Wang, Y.; Ling, L.; Feng, X. Graphene-Based Porous Silica Sheets Impregnated with Polyethyleneimine for Superior CO_2 Capture. *Adv. Mater.* **2013**, *25*, 2130–2134.

18. Lee, W. H.; Park, J.; Sim, S. H.; Lim, S.; Kim, K. S.; Hong, B. H.; Cho, K. Surface-Directed Molecular Assembly of Pentacene on Monolayer Graphene for High-Performance Organic Transistors. *J. Am. Chem. Soc.* **2011**, *133*, 4447–4454.

19. Ou, X.; Jiang, L.; Chen, P.; Zhu, M.; Hu, W.; Liu, M.; Zhu, J.; Ju, H. Highly Stable Graphene-Based Multilayer Films Immobilized *via* Covalent Bonds and Their Applications in Organic Field-Effect Transistors. *Adv. Funct. Mater.* **2013**, *23*, 2422–2435.

20. Nam, S.; Jang, J.; Kim, K.; Yun, W. M.; Chung, D. S.; Hwang, J.; Kwon, O. K.; Chang, T.; Park, C. E. Solvent-Free Solution Processed Passivation Layer for Improved Long-Term Stability of Organic Field-Effect Transistors. *J. Mater. Chem.* **2011**, *21*, 775–780.

21. Sekitani, T.; Zschieschang, U.; Klauk, H.; Someya, T. Flexible Organic Transistors and Circuits with Extreme Bending Stability. *Nat. Mater.* **2010**, *9*, 1015–1022.

22. Yang, H.; Yang, L.; Ling, M.-M.; Lastella, S.; Gandhi, D. D.; Ramanath, G.; Bao, Z.; Ryu, C. Y. Aging Susceptibility of Terrace-like Pentacene Films. *J. Phys. Chem. C* **2008**, *112*, 16161–16165.

23. Schaer, M.; Nüesch, F.; Berner, D.; Leo, W.; Zuppiroli, L. Water Vapor and Oxygen Degradation Mechanisms in Organic Light Emitting Diodes. *Adv. Funct. Mater.* **2001**, *11*, 116–121.

24. Li, D.; Borkent, E.-J.; Nortrup, R.; Moon, H.; Katz, H.; Bao, Z. Humidity Effect on Electrical Performance of Organic Thin-Film Transistors. *Appl. Phys. Lett.* **2005**, *86*, 042105.

25. Jeon, H.; Shin, K.; Yang, C.; Park, C. E.; Park, S.-H. K. Thin-Film Passivation by Atomic Layer Deposition for Organic Field-Effect Transistors. *Appl. Phys. Lett.* **2008**, *93*, 163304.

26. Kim, N.; Potscavage, W. J.; Domercq, B.; Kippelen, B.; Graham, S. A hybrid Encapsulation Method for Organic Electronics. *Appl. Phys. Lett.* **2009**, *94*, 163308.

27. Meyer, J.; Görrn, P.; Bertram, F.; Hamwi, S.; Winkler, T.; Johannes, H.-H.; Weimann, T.; Hinze, P.; Riedl, T.; Kowalsky, W. Al_2O_3/ZrO_2 Nanolaminates as Ultrahigh Gas-Diffusion Barriers—A Strategy for Reliable Encapsulation of Organic Electronics. *Adv. Mater.* **2009**, *21*, 1845–1849.

28. Jang, J.; Nam, S.; Chung, D. S.; Kim, S. H.; Yun, W. M.; Park, C. E. High Tg Cyclic Olefin Copolymer Gate Dielectrics for N,N′-Ditridecyl Perylene Diimide Based Field-Effect Transistors: Improving Performance and Stability with Thermal Treatment. *Adv. Funct. Mater.* **2010**, *20*, 2611–2618.

29. Singh, T. B.; Marjanović, N.; Matt, G. J.; Günes, S.; Sariciftci, N. S.; Montaigne Ramil, A.; Andreev, A.; Sitter, H.; Schwödiauer, R.; Bauer, S. High-Mobility *n*-Channel Organic Field-Effect Transistors based on Epitaxially Grown C60 Films. *Org. Electron.* **2005**, *6*, 105–110.

30. Kim, K. S.; Zhao, Y.; Jang, H.; Lee, S. Y.; Kim, J. M.; Kim, K. S.; Ahn, J.-H.; Kim, P.; Choi, J.-Y.; Hong, B. H. Large-Scale Pattern Growth of Graphene Films for Stretchable Transparent Electrodes. *Nature* **2009**, *457*, 706–710.

31. Lange, P.; Dorn, M.; Severin, N.; Vanden Bout, D. A.; Rabe, J. P. Single- and Double-Layer Graphenes as Ultrabarriers for Fluorescent Polymer Films. *J. Phys. Chem. C* **2011**, *115*, 23057–23061.

32. Wang, Y.; Tong, S. W.; Xu, X. F.; Özyilmaz, B.; Loh, K. P. Interface Engineering of Layer-by-Layer Stacked Graphene Anodes for High-Performance Organic Solar Cells. *Adv. Mater.* **2011**, *23*, 1514–1518.

33. Chen, S.; Brown, L.; Levendorf, M.; Cai, W.; Ju, S.-Y.; Edgeworth, J.; Li, X.; Magnuson, C. W.; Velamakanni, A.; Piner, R. D. Oxidation Resistance of Graphene-Coated Cu and Cu/Ni Alloy. *ACS Nano* **2011**, *5*, 1321–1327.

34. Kato, Y.; Iba, S.; Teramoto, R.; Sekitani, T.; Someya, T.; Kawaguchi, H.; Sakurai, T. High Mobility of Pentacene Field-Effect Transistors with Polyimide Gate Dielectric Layers. *Appl. Phys. Lett.* **2004**, *84*, 3789–3791.

35. Meijer, E. J.; de Leeuw, D. M.; Setayesh, S.; van Veenendaal, E.; Huisman, B. H.; Blom, P. W. M.; Hummelen, J. C.; Scherf, U.; Klapwijk, T. M. Solution-Processed Ambipolar Organic Field-Effect Transistors and Inverters. *Nat. Mater.* **2003**, *2*, 678–682.

36. Vollmer, A.; Weiss, H.; Rentenberger, S.; Salzmann, I.; Rabe, J. P.; Koch, N. The Interaction of Oxygen and Ozone with Pentacene. *Surf. Sci.* **2006**, *600*, 4004–4007.

37. Jurchescu, O. D.; Baas, J.; Palstra, T. T. M. Electronic Transport Properties of Pentacene Single Crystals upon Exposure to Air. *Appl. Phys. Lett.* **2005**, *87*, 052102.

38. Son, D. I.; Kim, T. W.; Shim, J. H.; Jung, J. H.; Lee, D. U.; Lee, J. M.; Park, W. I.; Choi, W. K. Flexible Organic Bistable Devices Based on Graphene Embedded in an Insulating Poly(methyl methacrylate) Polymer Layer. *Nano Lett.* **2010**, *10*, 2441–2447.

39. Park, J. H.; Hwang, D. K.; Lee, J.; Im, S.; Kim, E. Studies on Poly(methyl methacrylate) Dielectric Layer for Field Effect Transistor: Influence of Polymer Tacticity. *Thin Solid Films* **2007**, *515*, 4041–4044.

40. Yun, W. M.; Jang, J.; Nam, S.; Jeong, Y. J.; Kim, L. H.; Park, S.; Seo, S. J.; Park, C. E. Vacuum Thermally Evaporated Polymeric Zinc Acrylate as an Organic Interlayer of Organic/Inorganic Multilayer Passivation for Flexible Organic Thin-Film Transistors. *J. Mater. Chem.* **2012**, *22*, 25395–25401.